UDK 519.61/.64:66.017:620.174:666.189.2
Original scientific article/Izvirni znanstveni članek

ISSN 1580-2949
MTAEC9, 50(1)23(2016)

INVESTIGATION OF HOLE EFFECTS ON THE CRITICAL BUCKLING LOAD OF LAMINATED COMPOSITE PLATES

PREISKAVA VPLIVA LUKNJE NA KRITIČNO UPOGIBNO OBREMENITEV LAMINIRANIH KOMPOZITNIH PLOŠČ

Ali Kurşun, Ersin Topal

Department of Mechanical Engineering, Hitit University, 19030 Çorum, Turkey
alikursun@hitit.edu.tr

Prejem rokopisa – received: 2014-08-01; sprejem za objavo – accepted for publication: 2015-03-04

doi:10.17222/mit.2014.164

In this study, the effects of the hole diameter on the buckling behavior of glass-fiber-reinforced, laminated composite rectangular plates were investigated both experimentally and numerically. As the test specimens, E-glass/epoxy symmetric-ply composites with eight layers were manufactured using the hand lay-up technique and drilled with different hole diameters ranging from 10 to 40 mm. The laminated composite plates were arranged with different symmetric orientation angles such as $[(0°/90°)_2]_s$, $[(-15°/15°)_2]_s$, $[(-30°/30°)_2]_s$ and $[(-45°/45°)_2]_s$. The experimental critical-buckling loads of the plates were found by clamping the bottom and upper edges and then these results were compared with the results obtained with the numerical analysis. The determination of the critical buckling loads for the laminated composite plates with different hole diameters was performed using the ANSYS 12.1® finite-element-analysis software. The numerical analysis showed good agreement with the experimental results for different hole diameters and fiber orientation angles. It was concluded that the critical buckling loads strongly depend on the diameter of the hole and fiber orientation angles.

Keywords: buckling, glass fibers, finite element method (FEM)

V tej študiji je bil eksperimentalno in numerično preiskovan vpliv premera luknje na obnašanje pri upogibu s steklenimi vlakni laminirane kompozitne štirioglate plošče. Kompozitni vzorci so bili izdelani s simetričnim polaganjem E-steklo/epoksi, z osmimi plastmi, z uporabo tehnike ročnega polaganja in vrtanja lukenj različnega premera od 10 do 40 mm. Laminirane kompozitne plošče so bile izdelane z različnimi, simetrično orientiranimi koti vlaken, $[(0°/90°)_2]_s$, $[(-15°/15°)_2]_s$, $[(-30°/30°)_2]_s$ in $[(-45°/45°)_2]_s$. Eksperimentalna kritična upogibna obremenitev plošč je bila ugotovljena z vpetjem spodnjega in zgornjega roba, rezultati pa so bili primerjani z rezultati numerične analize. Določitev kritične upogibne obremenitve za laminirane kompozitne plošče z luknjami z različnim premerom, je bila izvršena z uporabo programa za analizo končnih elementov ANSYS 12.1®. Numerična analiza je pokazala dobro ujemanje z rezultati preizkusov, za različne premere lukenj in orientacijske kote vlaken. Ugotovljeno je, da je kritična upogibna obremenitev močno odvisna od premera luknje in od kota orientacije vlaken.

Ključne besede: upogibanje, steklena vlakna, metoda končnih elementov (FEM)

1 INTRODUCTION

Fiber-reinforced composite plates are widely used in many types of engineering applications such as the aerospace, automotive and marine industries, as well as in medical prosthetic devices, electronic circuit boards and sports equipment because of certain properties such as high specific stiffness and strength. A plate which is subjected to an axial compressive load ought to remain stable. If, in spite of a small addition of an axial or lateral disturbance applied to a plate, it remains to be in equilibrium, then the plate is said to be stable. If a small additional disturbance results in a large response and the plate does not return to its original equilibrium configuration, the plate is said to be unstable.

The magnitude of the compressive axial load, at which the plate becomes unstable is called the critical buckling load. If the load is increased beyond this critical load, it results in a large deflection and the plate seeks another equilibrium configuration. Thus, the load at which a plate becomes unstable is of practical importance in the design of structural elements. One of the important issues is the prediction of the critical buckling loads of composite materials. Here we determine the critical buckling loads of the laminated composite rectangular plates with a cylindrical hole using experimental and numerical methods.

The buckling behavior of symmetric cross-ply and angle-ply laminated flat composite columns was described in[1], investigating the effects of the column thickness and wideness, the orientation angles, the fillet radius and the modulus ratios on the critical buckling load with the finite-element method (FEM) based on the first-order shear-deformation theory (FSDT). Arman et al.[2] investigated the effect of the delamination around a single circular hole on the critical buckling load of woven-fabric-laminated composite plates. Besides the critical buckling load, they determined the critical delamination diameter. A buckling analysis of a woven-glass-polyester and boron/epoxy laminated composite plate containing a circular/elliptical hole given in[3,4], respectively, was done using the FEM.

Aydogdu[5] studied the thermal-buckling behavior of cross-ply laminated beams, subjected to different boun-

dary conditions. He used the Ritz method to obtain the critical buckling temperatures. Kim and Lee[6] developed fine-beam elements named as 2-, 3- and 4-noded isoparametric beam elements to analyze the lateral buckling of the shear-deformable laminated composites. Jung and Han[7] presented an approach for the initial buckling behavior of laminated composite plates and shells subjected to the combined in-plane loading. Laurin et al.[8] developed an approach for the multiscale-failure behavior for various stacking sequences. The buckling response of laminated composite structures with a delamination was investigated by Lee and Park[9].

Matsunaga[10] used the method of the power series expansion of continuous-displacement components to come up with the two-dimensional global-deformation theory for the thermal buckling of laminated composites and sandwich plates. The thermal-buckling behavior of laminated hybrid-composite plates containing a hole, subjected to a uniform temperature was studied by Şahin[11]. The thermal-buckling mode shapes of laminated composites with varying fiber orientations, stacking sequences and $E1/E2$ ratios are studied in[12]. The thermo-mechanical-buckling response of laminated composites and sandwich plates was investigated by Wu and Chen[13].

The post- and thermal-buckling behavior of laminated composite beams with temperature-dependent material properties is given in[14]. Dash and Singh[15] developed an isoparametric nonlinear finite-element method for the buckling and post-buckling of laminated composite plates. The buckling behavior of a composite structure based on the generalized differential quadrature rule (GDQR) and Rayleigh-Ritz (R-R) method is presented in[16,17]. Topal and Uzman[18] investigated the optimization of the critical failure mode of simply supported laminated composite plates under in-plane static loads. Shufrin et al.[19] generated a semi-analytical formulation based on the total energy minimization and the iterative extended Kantorovich approach for the buckling analysis of symmetrically laminated composite plates. Malekzadeh and Shojaee[20] studied the buckling response of carbon-nanotube-reinforced, quadrilateral laminated plates. Özben[21] presented the critical buckling load for laminated composite plates using the FEM and analytical methods. The effects of the hole location and diameter on the lateral-buckling response of woven-fabric-laminated composite cantilever beams were determined experimentally and numerically in[22].

In this study, the effects of the hole diameter and fiber orientations on the buckling behavior of glass-fiber-reinforced, laminated composite rectangular plates were investigated experimentally and numerically under compression. Firstly, the test specimens for different fiber orientation angles were prepared with and without the holes. The test specimens made of glass/epoxy consisted of eight symmetric plies. A uniformly distributed load was applied to the upper edges of the plate specimens and critical buckling loads were determined experimentally and numerically. The results obtained with the experimental and numerical methods were in good agreement. The results showed that the critical buckling loads strongly depend on the diameter of the hole and the fiber orientation angles.

2 MATERIALS AND METHODS

2.1 Test specimens

For the experiments, laminated composite plates consisting of eight layers of e-glass woven fabrics with various fiber orientation angles such as $[(0°/90°)_2]_s$, $[(-15°/15°)_2]_s$, $[(-30°/30°)_2]_s$ and $[(-45°/45°)_2]_s$ were manufactured. The fiber volume fraction and the nominal thickness of the composite were approximately 55 % and 2 mm, respectively. For the matrix material, the CY225 epoxy resin and hardener HY225 were used. The curing process was implemented at 120 °C for 3 h under a pressure of 0.25 MPa.[23] Then, the composite was cooled to room temperature. The prepared plates were cut to the dimensions of 100 × 100 mm and drilled in the center with different hole diameters such as 0 (without a hole), 10, 20, 30 and 40 mm respectively. **Table 1** shows the mechanical properties of the laminated composites.

Table 1: Mechanical properties of the composites plate
Tabela 1: Mehanske lastnosti kompozitnih plošč

$E_1 = E_2$ (GPa)	E_3 (GPa)	$G_{12} = G_{13} = G_{23}$ (GPa)	ν_{12}	$\nu_{13} = \nu_{23}$
28.500	17.100	7.840	0.148	0.088

2.2 Experimental procedure of the critical buckling load

The buckling tests were done in the compression mode on a Shimadzu AG-100 kN test machine. The buckling-test apparatus designed by Arman et al.[2] consists of two clamped edges at the bottom and top and two free edges as the boundary conditions as shown in **Figure 1**. As a result of the clamped boundary condition of the buckling-test apparatus that holds the specimen at the bottom and top edges, each having a 10 mm

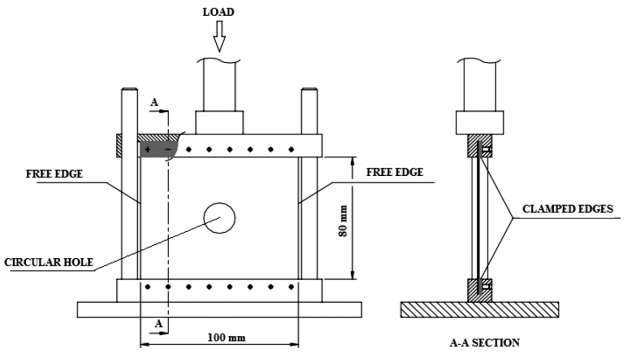

Figure 1: Buckling-test apparatus[2]
Slika 1: Naprava za upogibni preizkus[2]

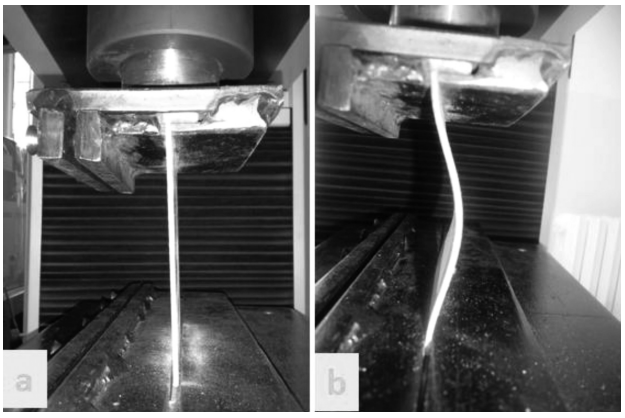

Figure 2: View of the buckling-test process: a) before buckling and b) after buckling
Slika 2: Izgled upogibnega preizkusa: a) pred upogibanjem, b) po upogibanju

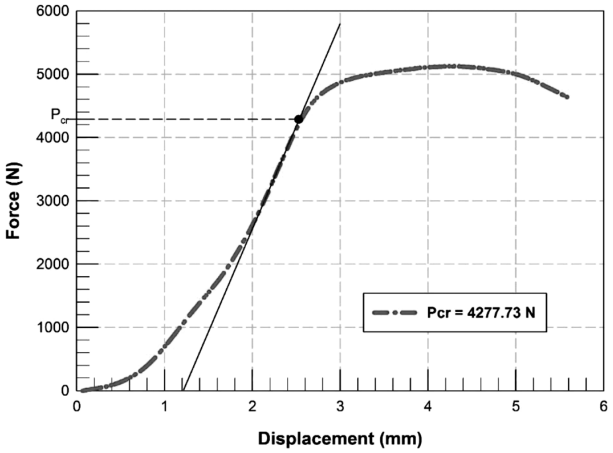

Figure 3: Determination of the experimental critical buckling load
Slika 3: Eksperimentalno določanje kritične upogibne obremenitve

clamping length, the height of the test specimens were determined to be 80 mm as shown in **Figure 1**.

Three identical specimens were tested for each hole diameter and all the specimens were subjected to an axial compressive load until the first buckling mode was reached as shown in **Figure 2**. The laminated plate became unstable as the first buckling mode was reached. The magnitude of the axial compressive load, at which the plate becomes unstable, is called the critical buckling load. The other buckling modes were not studied in this paper.

The test results were taken as a text file on the data card of the test machine. Then the graphs of the load-displacement variations were created for each specimen. A MATLAB® code was written for the upheaval of the slope of the load-displacement curve. The critical buckling load was determined accordingly and shown in **Figure 3**. In this figure, P_{cr} is the critical buckling load.

2.3 Finite-element buckling model

A three-dimensional finite-element analysis of the composite plates with a single circular hole was performed using the commercial finite-element software ANSYS® 12.1. The model consists of eight layers with dimensions of 100 × 100 × 0.25 mm for each layer and the 2 mm total thickness of the plate. The diameter of the hole changes from 0 (without hole) to 10, 20, 30 and 40 mm. Additionally, the fiber orientation changes from $[(0°/90°)_2]_s$ to $[(–15°/15°)_2]_s$, $[(–30°/30°)_2]_s$ and $[(–45°/45°)_2]_s$. Therefore, a total of 20 models were constructed. After the modeling of the composite plates with a circular hole, the number of layers, the element type, the material properties of the laminated composite plates, the fiber orientation angles and the thickness of each layer were introduced to the finite-element program. The element type was a SHELL layered element having six degrees of freedom at each node: the translations in the nodal *x*, *y* and *z* directions and the rotations about the nodal *x*, *y* and *z* axes. Finally, for the analysis, the unit pressure was applied to one of the clamped edges, the model was meshed and the program was run.

3 RESULTS AND DISCUSSION

The critical-buckling-load results were obtained both experimentally and numerically for the $[(0°/90°)_2]_s$, $[(–15°/15°)_2]_s$, $[(–30°/30°)_2]_s$ and $[(–45°/45°)_2]_s$ fiber orientations for all the buckling-test specimens having 0 (without hole), 10, 20, 30 and 40 mm hole diameters, respectively. The experimental results for each hole diameter are presented in **Figure 4**. In this figure, three identical experimental graphs and their average values are shown.

It is clear that all the repeated experimental tests for each group with various hole-diameter values show a very similar buckling behavior as reported in **Figures 4a** to **4e**.

The average values of all the results obtained experimentally and numerically are given in **Table 2** in order to compare them in terms of the critical buckling load. In the same table, P^*_{cr} refers to the critical buckling load for the specimen without a hole.

Table 2: Critical buckling loads for numerical and experimental studies
Tabela 2: Kritična upogibna obremenitev pri numerični študiji in pri preizkusu

Hole diameter (mm)	Critical buckling loads (P_{cr}, P^*_{cr}) (N)							
	Fiber orientations (°)							
	$[(0°/90°)_2]_s$		$[(–15°/15°)_2]_s$		$[(–30°/30°)_2]_s$		$[(–45°/45°)_2]_s$	
	Exp.	Num.	Exp.	Num.	Exp.	Num.	Exp.	Num.
0	4867.2	4497.0	4347.3	4296.3	4000.7	4023.0	3660.1	3853.0
10	4310.5	4261.5	4277.7	4155.4	3934.1	3891.8	3540.8	3734.4
20	4194.7	4073.5	3896.2	3970.9	3700.6	3709.1	3140.3	3550.0
30	3710.9	3758.9	3703.3	3666.9	3434.5	3424.4	2830.7	3272.2
40	3326.3	3365.3	3117.8	3279.2	3034.3	3050.5	2280.9	2905.4

In addition, the experimental and numerical results showing the variation in the critical buckling load versus the hole diameter were presented in **Figure 5**. It is clear

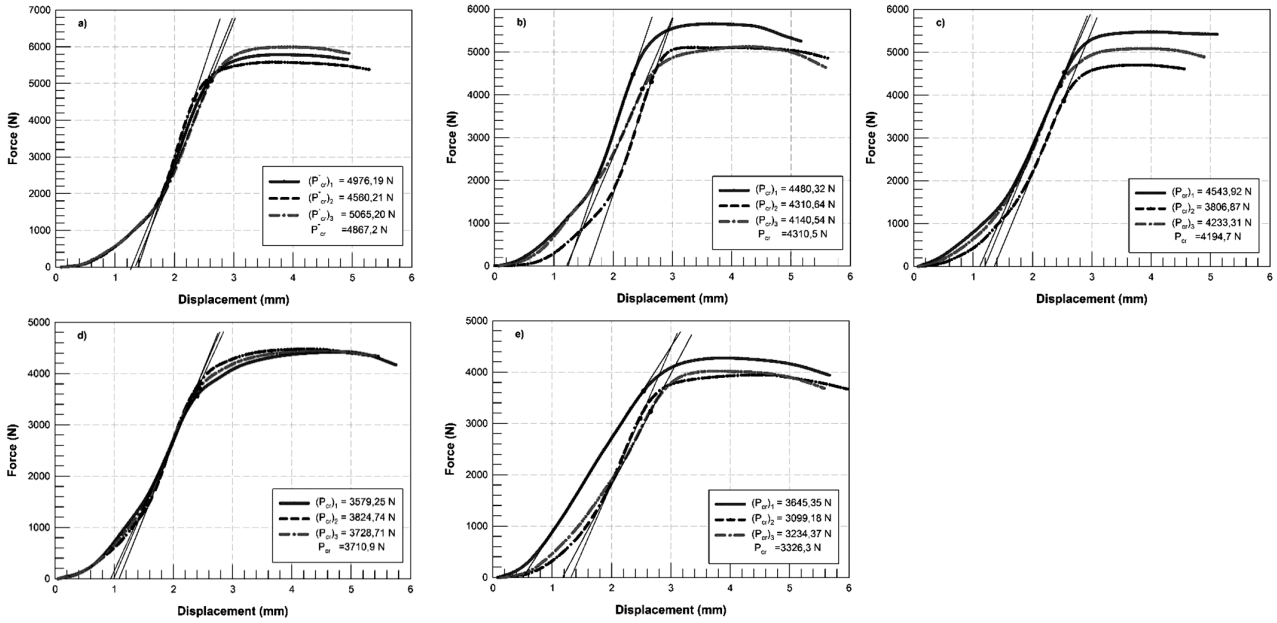

Figure 4: Experimental critical buckling loads for: a) without a hole, b) 10 mm hole diameter, c) 20 mm hole diameter, d) 30 mm hole diameter and e) 40 mm hole diameter

Slika 4: Eksperimentalne kritične upogibne obremenitve pri: a) brez luknje, b) premer luknje 10 mm, c) premer luknje 20 mm, d) premer luknje 30 mm in e) premer luknje 40 mm

from this figure that the experimental and numerical results are consistent with each other. **Figures 5** and **6** were automatically scaled starting at buckling loads of 1000 N and 2800 N, respectively, in order to clarify the difference between of the results.

From **Table 2** and **Figure 5**, it is concluded that the critical buckling load for all the types of fiber orientation angle has the highest value for the specimens without a hole and the lowest value for the specimens having a 40 mm hole diameter.

Figure 6 shows the variation in the critical buckling load versus the hole diameter in terms of fiber orientation. The critical buckling load for the same hole diameter is maximum at the orientation angle of $[(0°/90°)_2]_s$ and it decreases with the order of $[(–15°/15°)_2]_s$, $[(–30°/30°)_2]_s$ and $[(–45°/45°)_2]_s$ as reported in **Figure 6**. And also, the critical buckling load gradually decreases, while the hole diameter increases for all the types of fiber orientation.

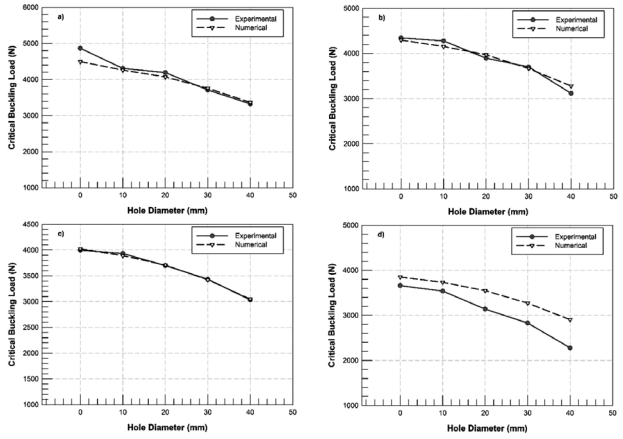

Figure 5: Comparison between the experimental and numerical results for fiber orientations: a) $[(0°/90°)_2]_s$, b) $[(–15°/15°)_2]_s$, c) $[(–30°/30°)_2]_s$ and d) $[(–45°/45°)_2]_s$

Slika 5: Primerjava rezultatov preizkusov in numeričnih rezultatov pri orientaciji vlaken: a) $[(0°/90°)_2]_s$, b) $[(–15°/15°)_2]_s$, c) $[(–30°/30°)_2]_s$ in d) $[(–45°/45°)_2]_s$

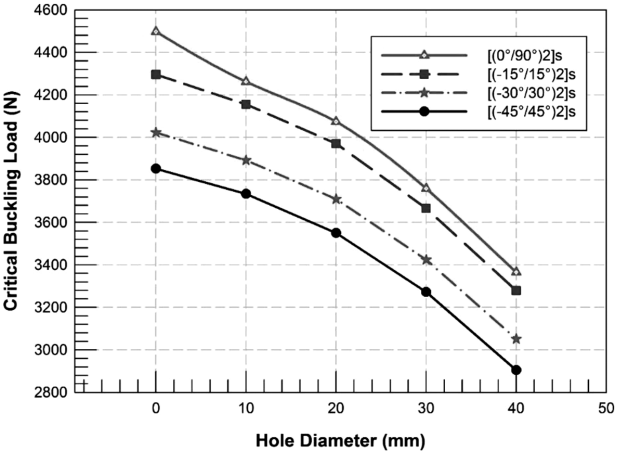

Figure 6: Numerical results for the critical buckling load versus the hole diameter for all types of fiber orientation

Slika 6: Numerični rezultati za kritično upogibno obremenitev v odvisnosti od premera luknje, pri vseh orientacijah vlaken

4 CONCLUSION

In this study, the buckling response of the composite plates with symmetric orientation angles such as $[(0°/90°)_2]_s$, $[(–15°/15°)_2]_s$, $[(–30°/30°)_2]_s$ and $[(–45°/45°)_2]_s$ with a single circular hole were examined by employing an experimental study and a numerical analysis performed with the finite-element technique. The conclusions that can be made in the contribution are as follows:

- The critical buckling loads are strongly dependent on the hole size for all the types of fiber orientation.
- The maximum values of the critical buckling load were obtained for the specimens with the $[(0°/90°)_2]_s$ orientation angle.
- The buckling load decreases exponentially with a decrease in the fiber orientation angle of the composite material.

5 REFERENCES

[1] H. Akbulut, O. Gundogdu, M. Şengül, Finite Elements in Analysis and Design, 46 (**2010**) 12, 1061–1067, doi:10.1016/j.finel.2010.07.004

[2] Y. Arman, M. Zor, S. Aksoy, Composites Science and Technology, 66 (**2006**) 15, 2945–2953, doi:10.1016/j.compscitech.2006.02.014

[3] M. Aydin Komur, F. Sen, A. Ataş, N. Arslan, Advances in Engineering Software, 41 (**2010**) 2, 161–164, doi:10.1016/j.advengsoft.2009.09.005

[4] D. Ouinas, B. Achour, Composites Part B: Engineering, 55 (**2013**), 575–579, doi:10.1016/j.compositesb.2013.07.011

[5] M. Aydogdu, Composites Science and Technology, 67 (**2007**) 6, 1096–1104, doi:10.1016/j.compscitech.2006.05.021

[6] N. I. Kim, J. Lee, International Journal of Mechanical Sciences, 68 (**2013**), 246–257, doi:10.1016/j.ijmecsci.2013.01.023

[7] W. Y. Jung, S. C. Han, Composite Structures, 109 (**2014**), 119–129, doi:10.1016/j.compstruct.2013.10.055

[8] F. Laurin, N. Carrere, J. F. Maire, Composite Structures, 80 (**2007**) 2, 172–182, doi:10.1016/j.compstruct.2006.04.074

[9] S. Y. Lee, D. Y. Park, International Journal of Solids and Structures, 44 (**2007**) 24, 8006–8027, doi:10.1016/j.ijsolstr.2007.05.023

[10] H. Matsunaga, Composite Structures, 68 (**2005**) 4, 439–454, doi:10.1016/j.compstruct.2004.04.010

[11] Ö. S. Şahin, Composites Science and Technology, 65 (**2005**) 11–12, 1780–1790, doi:10.1016/j.compscitech.2005.03.007

[12] L. C. Shiau, S. Y. Kuo, C. Y. Chen, Composite Structures, 92 (**2010**) 2, 508–514, doi:10.1016/j.compstruct.2009.08.035

[13] Z. Wu, W. Chen, International Journal of Mechanical Sciences, 49 (**2007**) 6, 712–721, doi:10.1016/j.ijmecsci.2006.10.006

[14] A. R. Vosoughi, P. Malekzadeh, Ma. R. Banan, Mo. R. Banan, International Journal of Non-Linear Mechanics, 47 (**2012**) 3, 96–102, doi:10.1016/j.ijnonlinmec.2011.11.009

[15] P. Dash, B. N. Singh, Mechanics Research Communications, 46 (**2012**), 1–7, doi:10.1016/j.mechrescom.2012.08.002

[16] M. Darvizeh, A. Darvizeh, R. Ansari, C. B. Sharma, Composite Structures, 63 (**2004**) 1, 69–74, doi:10.1016/s0263-8223(03)00133-8

[17] Y. Tang, X. Wang, International Journal of Mechanical Sciences, 53 (**2011**) 2, 91–97, doi:10.1016/j.ijmecsci.2010.11.005

[18] U. Topal, Ü. Uzman, Thin-Walled Structures, 45 (**2007**) 7–8, 660–669, doi:10.1016/j.tws.2007.06.002

[19] I. Shufrin, O. Rabinovitch, M. Eisenberger, Composite Structures, 82 (**2008**) 4, 521–531, doi:10.1016/j.compstruct.2007.02.003

[20] P. Malekzadeh, M. Shojaee, Thin-Walled Structures, 71 (**2013**), 108–118, doi:10.1016/j.tws.2013.05.008

[21] T. Özben, Computational Materials Science, 45 (**2009**) 4, 1006–1015, doi:10.1016/j.commatsci.2009.01.003

[22] E. Eryiğit, M. Zor, Y. Arman, Composites Part B: Engineering, 40 (**2009**) 2, 174–179, doi:10.1016/j.compositesb.2008.07.005

[23] A. Kursun, M. Senel, Experimental Techniques, 37 (**2013**) 6, 41–48, doi:10.1111/j.1747-1567.2011.00738.x